Prognostic and Diagnostic Modes of Mathematical Model for the Pre-operation of Suspended Sediment Transport model in Estuaries and Coastal areas

Worachat Wannawong, Chaiwat Ekkawatpanit, and Sanit Wongsa

Abstract—Both prognostic and diagnostic modes of a 3D baroclinic model in hydrodynamic and sediment transport models of the Princeton Ocean Model (POM) were conducted to separate prognose and diagnose effects of different hydrodynamic factors on transport of suspended sediment discharged from the rivers to the Gulf of Thailand (GoT). Both transport modes of suspended sediment distribution in the GoT were numerically simulated. It could be concluded that the suspended sediment discharged from the rivers around the GoT. Most of sediments in estuaries and coastal areas are deposited outside the GoT under the condition of wind-driven current, and very small amount of the sediments of them are transported faraway. On the basis of wind forcing, sediments from the lower GoT to the upper GoT are mainly transported south-northwestward and also continuously moved north-southwestward. An obvious 3D characteristic of suspended sediment transport is produced in the wind-driven current residual circulation condition. In this study, the transport patterns at the third layer are generally consistent with the typhoon-induced strong currents in two case studies of Typhoon Linda 1997. The case studies presented the prognostic and diagnostic modes during 00UTC28OCT1997 to 12UTC06NOV1997 in a short period with the current condition for pre-operation of the suspended sediment transport model in estuaries and coastal areas.

Keywords—prognostic, diagnostic, baroclinic, sediment transport, estuaries.

I. Introduction

THE management of regional sediments of the Gulf of Thailand (GoT) is being study by several Thai researchers. Historically, sediment studies were isolated to individual projects along a limited stretch of shoreline. This study, however, recognizes that the sediment management must be addressed on a regional basis because engineering activities or constructions that influence sediment processes in one location can have unforeseen consequences tens or hundreds of kilometers away. Managing sediment to benefit a region will save money, allow use of natural processes to solve engineering problems, and improve recreation resources and natural habitat. One goal for the regional sediment management program in the next few years is to initiate beneficial use

W. Wannawong is with the Earth System Science Cluster, The Joint Graduate School of Energy and Environment, King Mongkut's University of Technology Thonburi, Bangkok 10140, Thailand. e-mail: worachataj@hotmail.com, worachat.wan@kmutt.ac.th.

C. Ekkawatpanit is with the Department of Civil Engineering, Faculty of Engineering, King Mongkut's University of Technology Thonburi, Bangkok 10140, Thailand. e-mail: chaiwat.ekk@kmutt.ac.th.

S. Wongsa is with the Department of Civil Technology Education, Faculty of Industrial Education and Technology, King Mongkut's University of Technology Thonburi, Bangkok 10140, Thailand. e-mail: sanitwongsa@yahoo.com, sanit.won@kmutt.ac.th

Manuscript received August 1, 2011; revised September 23, 2011.

of dredged material for ecosystem restoration projects along the GoT shoreline.

As part of defining existing conditions for these projects, the authors which are supported by the Higher Education Research Promotion and National Research University Project of Thailand conducted an assessment of sediment sources and sinks, physical processes, and longshore transport in estuaries and coastal areas of the GoT. This study, the assessment compiles information by both prognostic and diagnostic modes of the 3D baroclinic model in the hydrodynamic and sediment transport models of the Princeton Ocean Model (POM)[1].

The pre-operation of suspended sediment transport model in estuaries and coastal areas of the GoT are designed to study in the cases of storm currents presented in the ocean current of 3D prognostic and diagnostic modes of the POM model. It is designed to solve the governing equation for transport phenomena under the surface boundary condition by the mathematical modeling. The mathematical modeling of the POM model describes the Reynold's averaged equations of mass, momentum, temperature and salinity conservations that are called the primitive equation. The POM model has been developed to study the external gravity waves, internal gravity waves, tidal waves, surges and currents. In recent years, wind-waves and storm surges generated by tropical cyclones in the GoT region have been studied using the modified WAve Model Cycle 4 (WAMC4) and POM model. Wannawong et al. [13], [14], [15], [17], [18] compared the results of WAMC4 and POM model with the observed data, and found that the model results were consistent with the best track data of Typhoon Linda, 1997 [12], [19] obtained from the Joint Typhoon Warning Center (JTWC) database of best track data. They also studied the comparison of orthogonal curvilinear grid and orthogonal rectangular grid in the horizontal coordinates [10], and concluded that the storm surge and current could be studied by the orthogonal rectangular grid.

The objective of this study is to modify the prognostic and diagnostic modes of the POM model in order to pre-operate the suspended sediment transport model in estuaries and coastal areas. The domain used in this study was extended from the study domain in the previous work of Wannawong et al. [10]. In this study, the domain was also applied to study the storm currents of Typhoon Linda by the POM model. The domain covering from $99°E$ to $111°E$ in longitude and from $2°N$ to $14°N$ in latitude [13] was applied to both experiments; 3D baroclinic model in the prognostic and in the diagnostic options. The outline of this study is organized as follows: Section

II gives a brief description of the mathematical modeling and its governing equation; Section III presents the model setting and parameterizations; Section IV shows the experimental design and results; and Section V presents the discussion and conclusion of this study.

II. MATHEMATICAL MODELING AND ITS GOVERNING EQUATION

The mathematical model used in the present study has been operated in the Earth System Science laboratory, King Mongkut's University of Technology Thonburi. It was developed from the POM model [1] to predict the storm surges, inundations, currents, suspended sediment transport in estuaries and coastal circulations. In this section, a brief description of the model applying in the GoT is given. The governing equation of the hydrodynamic model can be described as in the system of orthogonal Cartesian coordinates consist of the Reynold's averaged equations of mass, momentum, and temperature and salinity conservations. The equations include the effect of the gravitational/buoyancy forces as well as the effect of the Coriolis pseudo–force which are shown in this section.

Continuity equation:

$$\frac{\partial u}{\partial x} + \frac{\partial v}{\partial y} + \frac{\partial w}{\partial z} = 0, \tag{1}$$

x–momentum equation:

$$\frac{\partial u}{\partial t} + \frac{\partial (u^2)}{\partial x} + \frac{\partial (uv)}{\partial y} + \frac{\partial (uw)}{\partial z} = -\frac{1}{\rho_\circ}\frac{\partial p}{\partial x}$$
$$+ fv + \frac{\partial}{\partial z}\left(A_{mv}\frac{\partial u}{\partial z}\right) + F_x, \tag{2}$$

y–momentum equation:

$$\frac{\partial v}{\partial t} + \frac{\partial (uv)}{\partial x} + \frac{\partial (v^2)}{\partial y} + \frac{\partial (vw)}{\partial z} = -\frac{1}{\rho_\circ}\frac{\partial p}{\partial y}$$
$$- fu + \frac{\partial}{\partial z}\left(A_{mv}\frac{\partial v}{\partial z}\right) + F_y, \tag{3}$$

z–momentum or hydrostatic equation:

$$\frac{\partial p}{\partial z} = -\rho g, \tag{4}$$

Temperature equation:

$$\frac{\partial T}{\partial t} + \frac{\partial (uT)}{\partial x} + \frac{\partial (vT)}{\partial y} + \frac{\partial (wT)}{\partial z} =$$
$$\frac{\partial}{\partial z}\left(A_{hv}\frac{\partial T}{\partial z}\right) + F_T, \tag{5}$$

Salinity equation:

$$\frac{\partial S}{\partial t} + \frac{\partial (uS)}{\partial x} + \frac{\partial (vS)}{\partial y} + \frac{\partial (wS)}{\partial z} =$$
$$\frac{\partial}{\partial z}\left(A_{hv}\frac{\partial S}{\partial z}\right) + F_S, \tag{6}$$

The terms F_x, F_y, F_T and F_S found in the equations (2), (3), (5), and (6) represent the unresolved processes and in analogy to molecular diffusion. These terms can be written as

$$F_x = \frac{\partial}{\partial x}\left[2A_m\frac{\partial u}{\partial x}\right] + \frac{\partial}{\partial y}\left[A_m\left(\frac{\partial u}{\partial y} + \frac{\partial v}{\partial x}\right)\right],$$

$$F_y = \frac{\partial}{\partial y}\left[2A_m\frac{\partial v}{\partial y}\right] + \frac{\partial}{\partial x}\left[A_m\left(\frac{\partial u}{\partial y} + \frac{\partial v}{\partial x}\right)\right],$$

and

$$F_{T,S} = \frac{\partial}{\partial x}A_h\frac{\partial (T,S)}{\partial x} + \frac{\partial}{\partial y}A_h\frac{\partial (T,S)}{\partial y}.$$

where u, v are the horizontal components of the velocity vector ($m\ s^{-1}$), w is the vertical component of the velocity vector ($m\ s^{-1}$), g is the gravitational acceleration ($m\ s^{-2}$), p is the local pressure (Pa), $\rho(x, y, z, t, T, S)$ is the local density ($kg\ m^{-3}$), $\rho_\circ$ is the reference water density ($kg\ m^{-3}$), A_m is the horizontal turbulent diffusion coefficient ($m^2\ s^{-1}$), A_{mv} is the vertical turbulent diffusion coefficient ($m^2\ s^{-1}$), $f = 2\Omega\sin\phi$ is the Coriolis parameter where Ω is the speed of angular rotation of the Earth by $\Omega = 7.2921 \times 10^{-5}\ rad\ s^{-1}$ and ϕ is the latitude (° or degree), T is the potential temperature (°C), S is the potential salinity (psu), A_h is the horizontal thermal diffusivity coefficient ($m^2\ s^{-1}$), A_{hv} is the vertical thermal diffusivity coefficient ($m^2\ s^{-1}$), F_x and F_y are the horizontal viscosity terms and F_T and F_S are the horizontal diffusion terms of temperature and salinity, respectively.

The main assumptions used in the derivation of the above equations are that: (a) the water is incompressible ($D\rho/Dt = 0$); (b) the differences of density are small and can be neglected, except in buoyant forces (Boussinesq approximation). Consequently, the density $\rho_\circ$ used in the x and y momentum in the equations (2) and (3) is a reference density that is either represented by the standard density of the water or by the depth averaged water density as follows:

$$\rho_\circ = \frac{1}{\eta + h}\int_{-h}^{\eta}\rho dz = \frac{1}{D}\int_{-h}^{\eta}\rho dz \tag{7}$$

where the total depth D is expressed as: $D = \eta + h$ that is, the sum of the sea surface elevation η above the mean sea level (MSL) plus the depth h of the still water level. The density ρ used in the z momentum is represented by the sum of the reference density $\rho_\circ$ and its variation ρ' ($\rho = \rho_\circ + \rho'$); and (c) the vertical dimensions are much smaller than the horizontal dimensions of the water field and the vertical motions are also much smaller than the horizontal ones. Consequently, the vertical momentum equation reduces to the hydrostatic law (hydrostatic approximation) and the Coriolis term $2\Omega(v\sin\phi - w\cos\phi)$ reduces to $2\Omega v\sin\phi$ (see equation (2)). The vertical integration of the equation (4), from a depth z to the free surface η, yields the pressure at the water depth z as:

$$p|_\eta - p|_z = g\int_z^\eta\rho dz' \longrightarrow$$
$$p = p_{atm} + g\rho_\circ(\eta - z) + g\int_z^\eta\rho' dz' \tag{8}$$

where: z' is a dummy variable for the integration, η is the sea surface elevation above the mean sea level (MSL), $p|_z = p = p(x, y, z, t)$ and $p|_\eta = p_{atm} =$ Standard Atmospheric Pressure.

To close the above system of the continuity and motion equations, it is necessary to state the relationship of the water density, temperature and pressure. This relationship in the POM model is coded by the following formulation proposed

by Mellor [2], who did not only approximate the more general, but also the more computational expensive formulation of the International Equation of State (UNESCO):

$$\rho(S,T,p) = \rho(S,T,0) + \frac{p}{c^2}(1 - 0.20\frac{p}{c^2}) \cdot 10^4 \qquad (9)$$

$$c(S,T,p) = 1449.2 + 1.34(S - 35) + 4.55T - 0.045T^2$$
$$+ 0.00821p + 15.0 \cdot 10^{-9}p^2 \qquad (10)$$

where T is the temperature (°C), p is the gage pressure ($dbar$), S is the salinity (psu) and c is the speed of sound ($m\ s^{-1}$).

III. MODEL SETTING AND PARAMETERIZATIONS

A. Geometry of the study domain

The geometry of the study domain is defined by the shoreline, bathymetry, estuaries and coastal areas which also specified transfer boundaries. For the model run in covering of estuaries and coastal areas in the GoT, the computations take place on a $0.1° \times 0.1°$ rectilinear horizontal grid and on a sigma vertical grid (21 σ-layers). The domain covered from $99°E$ to $111°E$ in longitude and from $2°N$ to $14°N$ in latitude. The ocean current in the estuaries and coastal areas of the GoT on the $0.1° \times 0.1°$ grid was obtained from Geophysical Data Management System (GEODAS) of the NOAA National Geophysical Data Center (NGDC), Marine Geology (available online from http://www.ngdc.noaa.gov/mgg/gdas). The latest version of the ETOPO1, on a 1-minute latitude/longitude grid (1 minute of latitude = 1 nautical mile, or 1.853 km, updated on July 28, 2008 was used for the estuaries and coastal areas [4].

B. Model initialization and forcing

The model is initialized by setting the velocity, temperature and salinity fields to zero. The above set up known as "cold start" requires the model run for a spin up period before it reaches a state of statistical equilibrium. In the present application, a typhoon spin up period was adequate for the model to reach the equilibrium and to provide the realistic results. The forcing of model during the spin up period and the subsequent model simulations require the use of the following meteorological data: temperature, salinity, sea level pressure (Figure 3), and wind speed and its direction (Figure 2). The wind and pressure fields were obtained from the U.S. Navy Global Atmospheric Prediction System (NOGAPS) which is a global atmospheric forecast model with $1° \times 1°$ data resolution (Hogan and Rosmond [9]; Harr et al. [5]). The temperature and salinity [16] with $1° \times 1°$ data resolution provided by Levitus94 (Levitus and Boyer [7]; Levitus et al. [6]) were indicated by the climatological monthly mean fields in the model. The high resolution of $0.1° \times 0.1°$ spatial grid size gave 121×121 points by using the bilinear interpolation of these data in the horizontal coordinate [11]. In the vertical coordinate, 21 σ-levels were employed for adequacy and computational efficiency. The model time steps were 20 s and 1200 s (20 min) for the external and internal time steps, respectively.

The horizontal momentum equations consist of the local time derivative and horizontal advection terms, Coriolis deflection, sea level pressure gradient, tangential wind stress on the sea surface (Figure 4), and quadratic bottom friction. The system of equations is written in the flux form and solved by using the finite differential method that is centered in time and space on the Arakawa C grid. Finally, the results of Typhoon Linda from the POM were correspondingly represented two case studies in every hour. The prognostic and diagnostic modes of these case studies were operated during 0000 UTC on October 28, 1997 to 1200 UTC on November 6, 1997 with the current condition in order to pre-operate the model for suspended sediment transport in estuaries and coastal areas. The stability of the model was computed according to the CFL stability condition.

C. Prognostic and diagnostic descriptions

The POM model was applied in both 3D prognostic and diagnostic versions for suspended sediment transport testing in estuaries and coastal areas. The 3D internal calculating mode in both prognostic and diagnostic modes was used to predict the nearshore strong currents. For the vertically integrated current calculated by the POM model, the numerical experiments involving the use of circulation model in the prognostic and diagnostic modes in the 3D-internal mode have been performed. In the prognostic mode, the momentum equations as well as equations governing the temperature and salinity distributions were integrated as an initial value problem. These predictive experiments do not always reach the steady state since the oceanic response time for the density field can be considerable. As an alternative, diagnostic computations were considered. In the present study, the experiments were designed to simulate the currents in the prognostic and diagnostic modes which were referred to as Exp.I and Exp.II, respectively.

IV. EXPERIMENTAL DESIGN AND RESULTS

Typhoon Linda formed as the tropical disturbance on October 26, 1997 within an area of convection east of the Philippine Islands which is near $130°E$ in longitude and $10°N$ in latitude. It then moved westward under the subtropical ridge to the north. When entering the South China Sea (SCS), Typhoon Linda transformed into a tropical storm and moved westward to the southern tip of Cape Camau in Vietnam at 0900UTC on November 2, 1997 with the intensity of 28 $m\ s^{-1}$. After that, it approached the GoT at about 0030UTC on November 3 with typhoon intensity in a range of 33-42 $m\ s^{-1}$ and turned northwestward following steering from the subtropical ridge. Its strength weakened as it encountered mountains in Prachaubkirekhun province, Thailand. After crossing over the Andaman Sea, it reconsolidated and became typhoon once again at 0000UTC on November 6. In the present work, the study points considered along the best track are shown in Figure 1.

A. Experimental design

In order to compute the storm current at the third layer of 21 σ-levels, two experiments were performed (Table I). The
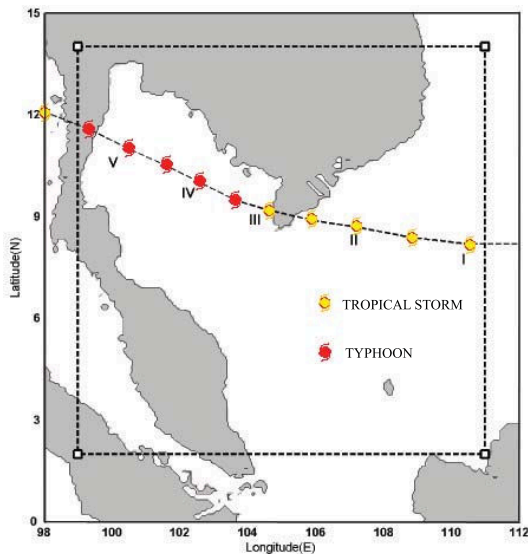
Fig. 1. Stations I, II, III, IV and V along the best track of Typhoon Linda 1997

hydrodynamic model used in this study was the POM model including the storm surge and current applications. In the 3D mode, the POM model was run by considering the difference between 3D prognostic and diagnostic modes. The model simulations were conducted utilizing the 3D prognostic and diagnostic modes of the POM model. To test the adequacy of the POM model, the 3D prognostic and diagnostic modes were tested as described above. The simulations of storm current were analyzed from a set of model experiments (Exp. I and Exp. II) in the short cycle with the current condition which was operated for the pre-operation of suspended sediment transport in estuaries and coastal areas. The descriptions of Exp. I and Exp. II are shown in Table I.

TABLE I
DESCRIPTION OF THE COMPUTATIONAL EXPERIMENTS

Experimental code	Description of computational experiments
Exp. I	3D baroclinic mode in the prognostic option
Exp. II	3D baroclinic mode in the diagnostic option

B. Results of experiments

The storm current generated by Typhoon Linda was firstly considered and computed by using the POM model (Exp. I). The storm currents related to the strong wind and low pressure (Figures 2–6) have been described by Bowden [3] and Pugh [8] relationships. The POM model used in both Exp. I and II was run by using the same wind field (wind speed), pressure field (sea level pressure), domain (wind fetch) and also the same time (duration), but with the different computational options. Figures 5 and 6 show the storm currents at the same location and time with the different optional calculation in the Exp. I. In the Exp. II, the difference of optional calculation at the third layer of 21 σ-levels can be easily considered in Figures

5 and 6, show the strong current of water recession in the 3D prognostic and diagnostic calculations for the pre-operation of suspended sediment transport model in estuaries and coastal areas.

The impacts of strong current and the difference between the minimum-maximum storm currents computed by the POM model at five locations of typhoon track were calculated (Figure 1 and Table II). The differences of storm currents at each station were presented in Table II. The maximum current speed at the station II was higher than others. It was 88.83 cm s^{-1} and 99.82 cm s^{-1} in the Exps. I and II, respectively. While the maximum current speed of Exp. I and II at the station IV was 66.99 and 99.08 cm s^{-1}, respectively. These results indicate that typhoon induced strong current were extreme in the SCS and then down in the GoT (Figure 7). In contrast, the wind speed of Typhoon Linda weakened in the SCS but it then became a strong wind in the GoT because of an influence of Super Typhoon Keith. The strong wind was peaked in the GoT as presented in the station V, whereas the extreme current was found in the SCS as shown in the station II. As the results found in this study, it could assume that the power of typhoon wind-wave could affect the erosion of the coastal areas around the GoT.

TABLE II
CURRENT SPEED COMPUTED BY THE POM MODEL ALONG THE POSITIONS
OF THE BEST TRACK OF TYPHOON LINDA 1997

Station	Date/time yymmddhh	JTWC		Computation (POM)	
		Position Lon., Lat. $^{\circ}E, ^{\circ}N$	WSP[1] Max. m/s	WSP[2] Min.-Max. m/s	Exp. I Min.-Max. cm/s	Exp. II Min.-Max. cm/s
I	97110112	110.5, 8.2	25.7	5.1-29.8	5.0-87.3	3.8-93.4
II	97110200	107.2, 8.7	28.3	4.1-28.3	2.0-88.8	17.2-99.8
III	97110212	104.6, 9.2	28.3	0.5-24.7	8.7-54.1	14.5-61.8
IV	97110300	102.6, 10.0	33.4	0.5-31.4	11.5-67.0	13.3-99.1
V	97110312	100.5, 11.0	33.4	0.5-33.4	9.6-52.9	10.5-87.9

[1] Wind speed of Typhoon track
[2] Wind speed of NOGAPS data

V. DISCUSSION AND CONCLUSION

To study the suspended sediment transport and wind-induced current in the GoT, the pre-operation of suspended sediment transport model in the POM model is necessary. The diagnostic mode showed the high impact with a stronger current than that shown in the prognostic mode. In this study, the results of currents at each station along the best track of Typhoon Linda (1997) predicted by the POM model were considered. The wind-induced current in this study demonstrate the impact of severe storm and also suspended sediment transport in the GoT. The results indicate that Typhoon Linda was the most severe storm and had high impact in estuaries and coastal areas of the GoT. Finally, the results of impacts of the storm currents obtained from this work will provide the necessary data to study the suspended sediment transport and also sediment morphological revolution in the future work.

REFERENCES

[1] A. F. Blumberg and G. L. Mellor, "A description of a threedimensional coastal ocean circulation model, In N. S. Heaps, editor, Three–dimensional coastal ocean models," *Coastal and estuarine sciences, American Geophysical Union*, vol. 4, pp. 1–16, 1987.

[2] G. L. Mellor, "An Equation of State for Numerical Models of Oceans and Estuaries," *Journal of Atmospheric and Oceanic Technology*, vol. 8, pp. 609–611, 1991.

[3] K. F. Bowden, *Physical Oceanography of Coastal Waters*, Ellis Horwood, Southampton, UK, 1983.

[4] C. Amante and B. W. Eakins, *1 ArcMinute Global Relief Model: Procedures, Data Sources and Analysis (ETOPO1)*, NOAA, National Geophysical Data Center, Boulder, Colorado, USA, 2008.

[5] P. Harr, R. Ellsberry, T. Hogan and W. Clune, "North Pacific cyclone sea–level pressure errors with NOGAPS," *Weather and Forecasting*, vol. 7, pp. 3–4, 1992.

[6] S. Levitus, R. Burgett and T. Boyer, *World Ocean Atlas: Salinity*, NOAA Atlas NESDIS 3, U. S. Government Printing Office, Washington DC, USA, vol.3, 1994.

[7] S. Levitus and T. Boyer, *World Ocean Atlas: Temperature*, NOAA Atlas NESDIS 4, U. S. Government Printing Office, Washington DC, USA, , vol.4, 1994.

[8] T. D. Pugh, *Tides, Surges and Mean Sea–Level*, a handbook for engineers and scientists, Chichester: John Wiley & Sons Inc., London, UK, 1987.

[9] T. F. Hogan and T. E. Rosmond, "The description of the Navy Operational Global Atmospheric System's spectral forecast model," *Monthly Weather Review*, vol. 119, pp. 1786–1815, 1991.

[10] W. Wannawong, U. W. Humphries and A. Luadsong, "The application of curvilinear coordinate for primitive equation in the Gulf of Thailand," *Thai Journal of Mathematics*, vol. 6, pp. 89–108, 2008.

[11] W. Wannawong, U. W. Humphries and P. Wongwises, "Optimization of bathymetry database for coastal areas," *Journal of Mathematics and Statistics*, vol. 6, pp. 286–293, 2010.

[12] W. Wannawong, U. W. Humphries, P. Wongwises, S. Vongvisessomjai and W. Lueangaram, "A two-dimensional wave prediction model along the best track of Typhoon Linda 1997," *American Journal of Environmental Sciences*, vol. 6, pp. 280–285, 2010.

[13] W. Wannawong, U. W. Humphries, P. Wongwises, S. Vongvisessomjai and W. Lueangaram, "A numerical study of two coordinates for energy balance equations by wave model," *Thai Journal of Mathematics*, vol. 8, pp. 197–214, 2010.

[14] W. Wannawong, U. W. Humphries, P. Wongwises, S. Vongvisessomjai and W. Lueangaram, "Numerical analysis of wave and hydrodynamic models for energy balance and primitive equations," *International Journal of Mathematical and Statistical Sciences*, vol. 4, pp. 140–150, 2010.

[15] W. Wannawong, U. W. Humphries, P. Wongwises, S. Vongvisessomjai and W. Lueangaram, "Numerical modeling and computation of storm surge for primitive equation by hydrodynamic model," *Thai Journal of Mathematics*, vol. 8, pp. 347–363, 2010.

[16] W. Wannawong, U. W. Humphries and P. Wongwises, "A study of temperature and salinity changes of seawater by mathematical modeling," *American-Eurasian Journal of Agricultural and Environmental Science*, vol. 4, pp. 446–451, 2010.

[17] W. Wannawong, U. W. Humphries, P. Wongwises and S. Vongvisessomjai, "Mathematical modeling of storm surge in three dimensional primitive equations," *International Journal of Computational and Mathematical Sciences*, vol. 1, pp. 44–53, 2010.

[18] W. Wannawong, U. W. Humphries, P. Wongwises and S. Vongvisessomjai, "Three steps of one-way nested grid for energy balance equation by wave model," *International Journal of Computational and Mathematical Sciences*, vol. 1, pp. 23–30, 2011.

[19] W. Wannawong, P. Wongwises, P. Ekphisutsuntorn, C. Ekkawatpanit and U. W. Humphries, "Numerical study of the effect of wind-waves generated by tropical cyclones using wave model: Storm surge and waves, Solutions to coastal disasters," *American Society of Civil Engineers (ASCE)*, vol. 1, pp. 149–163, 2011.

Worachat Wannawong received the B.Sc. degree in science–physics from Srinakharinwirot University, Bangkok, Thailand, in 2003, and the M.Sc. and Ph.D. degrees in applied mathematics from King Mongkuts University of Technology Thonburi (KMUTT), Bangkok, Thailand, in 2006 and 2010, respectively. He was with the Numerical Weather Prediction Center, Hydrographic Department, Royal Thai Navy from 2008 to 2010. He joined the Regional Ocean Modeling System (ROMS) team in October 2008. In April 2009, a part of his work was advised by Prof. Charitha Pattiaratchi and Prof. Krish Thiagarajan from the School of Environmental Systems Engineering and the School of Mechanical Engineering, University of Western Australia. In December 2009, he joined the workshop of the climate change project at KMUTT and Prof. Zhu Jiang from the Institute of Atmospheric Physics (IAP), Chinese Academy of Sciences, Beijing University gave him many ideas to modify the storm surge model by adjusting the drag coefficient. In 2011, He was a postdoctoral researcher at the earth system science cluster, the joint graduate school of energy and environment, KMUTT which supported by the Higher Education Research Promotion and National Research University Project of Thailand, Office of the Higher Education Commission and Center for Energy Technology and Environment, Ministry of Education, Thailand. He was visited with Prof. Ioannis Georgiou, Principle Investigator, Pontchartrain Institute for Environmental Sciences, Department of Earth and Environmental Sciences, University of New Orleans which gave him many ideas to develop the models to study the coastal erosive reduction, sediment transport and morphological evolution. His research interests involve numerical analysis, numerical weather prediction, computational mathematics, mathematical modelling, image processing and remote sensing in the fields of coastal erosive reduction, sediment transport and morphological evolution.

Chaiwat Ekkawatpanit received the B.Eng. and M.Eng. degrees in Water Resources Engineering from Kasetsart University and KMUTT, Bangkok, Thailand, in 1997 and 2001 respectively, and the Ph.D. degree in Civil and Environmental Engineering from Tohoku University, Sendai, Japan, in 2007. He currently is an water expert with the Department of Civil Engineering, Faculty of Engineering, KMUTT. He was the member of Japanese Society of Civil Engineers (JSCE) and Asia Pacific Association of Hydrology and Water Resources (APHW). His research interests include hydrological modeling, GIS, remote sensing, hydrology and watershed management, and impacts of climate change on water resources.

Sanit Wongsa received the B.Eng. and M.Eng. degrees in Civil Engineering from Kyushu Institute of Technology, Kyushu, Japan, in 1993 and 1995, and the Ph.D. degree in Environment and Resource Engineering from Hokkaido University, Hokkaido, Japan, in 2004, respectively. He currently is an Assistant Professor with the Department of Civil Technology Education, Faculty of Industrial Education and Technology, KMUTT. His research interests include computational fluid dynamics, flood modeling, numerical modeling and graphic programming.
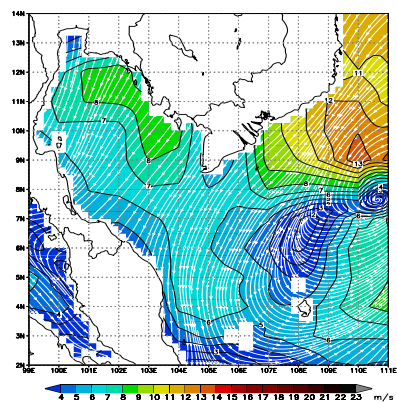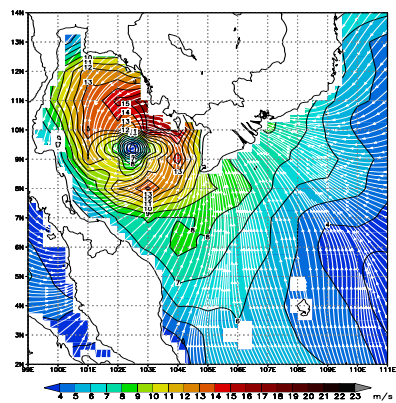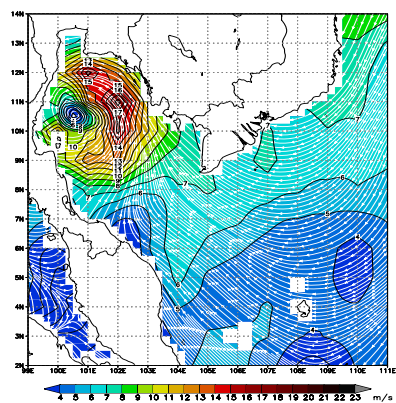
(a) 12UTC01NOV1997
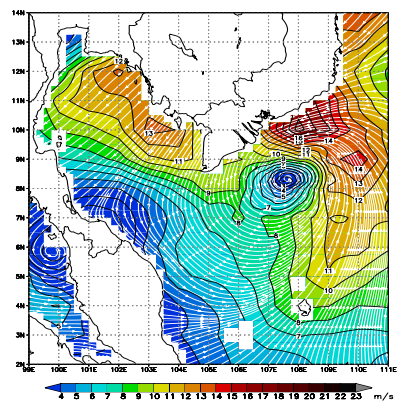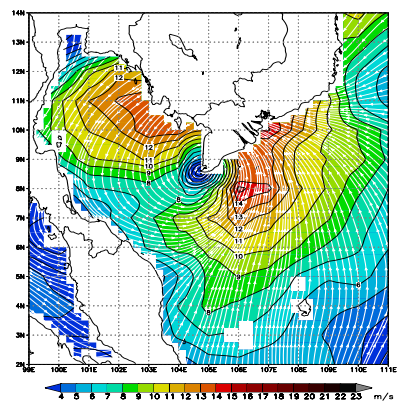
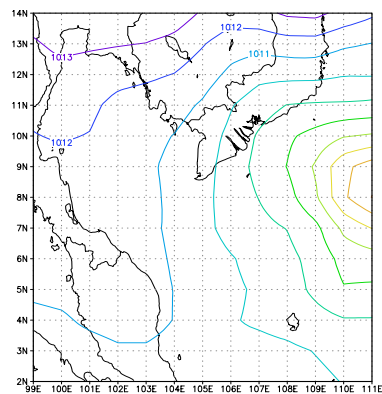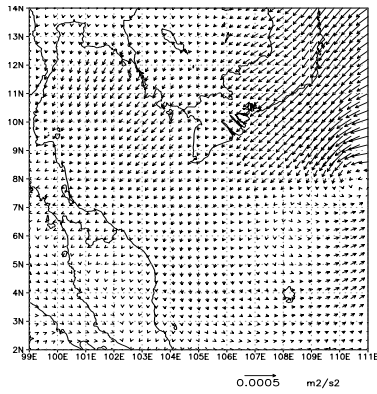(b) 00UTC02NOV1997

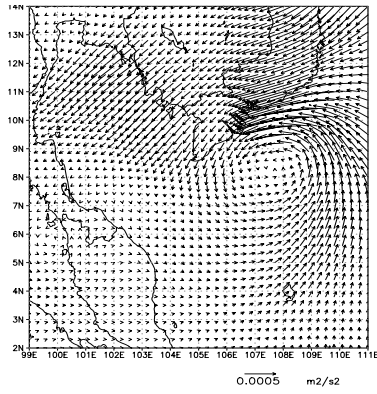(c) 12UTC02NOV1997

(d) 00UTC03NOV1997

(e) 12UTC03NOV1997

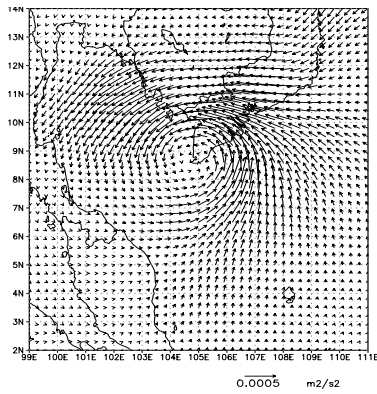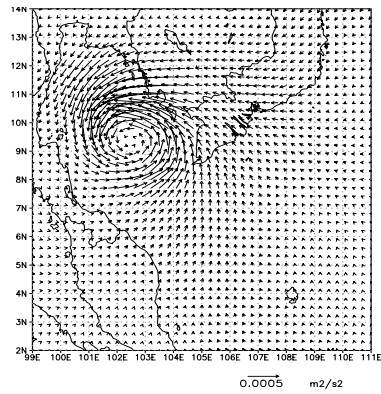Fig. 2. Wind streamline and speed ($m\ s^{-1}$) at the stations (a) I, (b) II, (c) III, (d) IV and (e) V
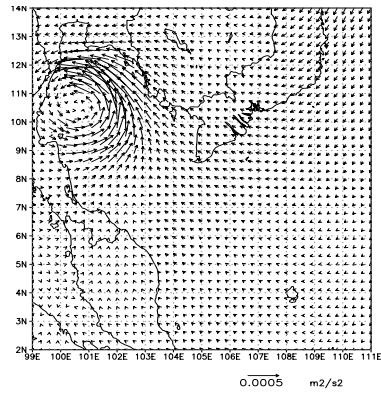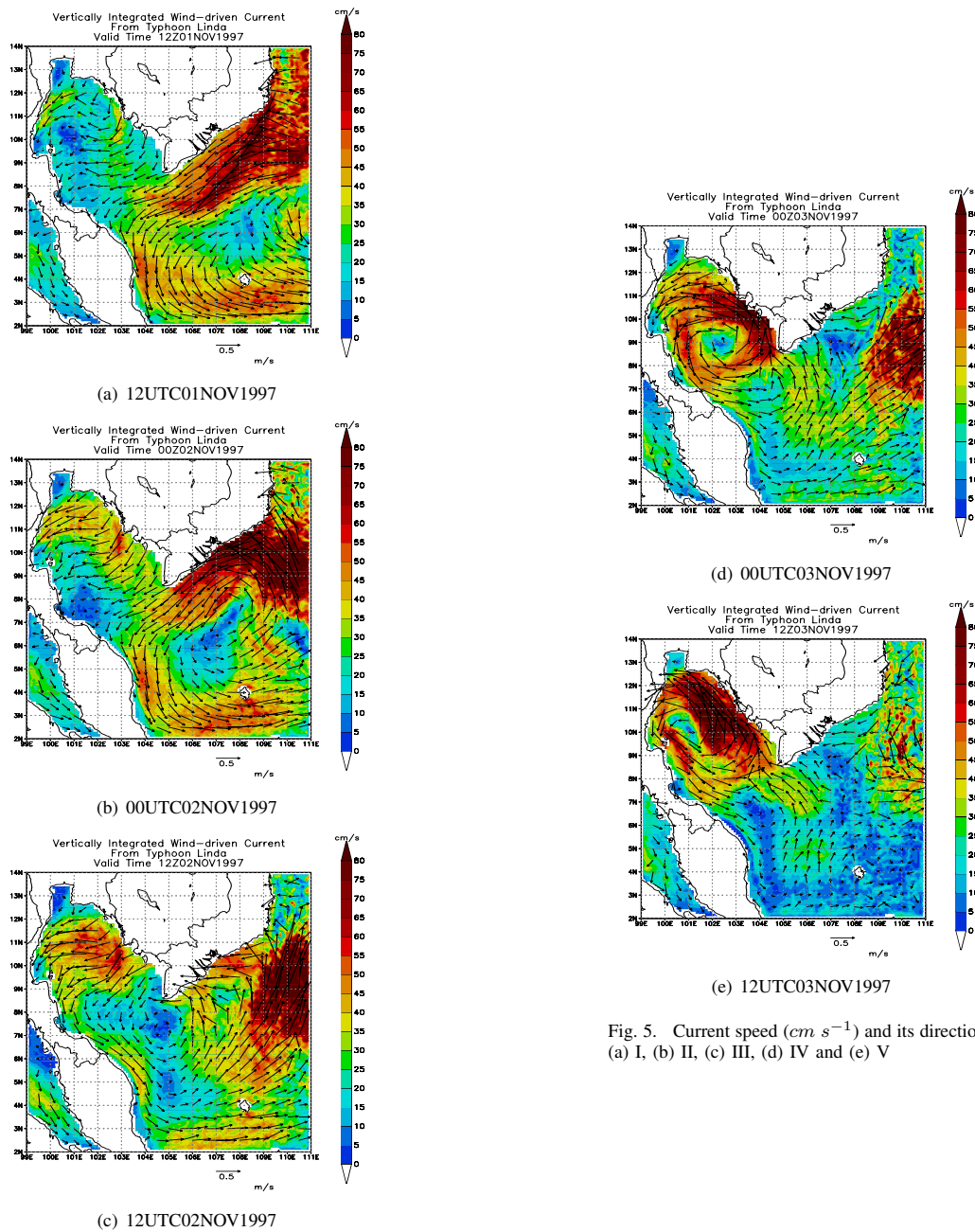
(a) 12UTC01NOV1997

(b) 00UTC02NOV1997

(c) 12UTC02NOV1997

(d) 00UTC03NOV1997

(e) 12UTC03NOV1997

Fig. 3. Sea level pressure (hPa) at the stations (a) I, (b) II, (c) III, (d) IV and (e) V

(a) 12UTC01NOV1997

(b) 00UTC02NOV1997

(c) 12UTC02NOV1997

(d) 00UTC03NOV1997

(e) 12UTC03NOV1997

Fig. 4. Wind stress ($m^2\ s^{-2}$) at the stations (a) I, (b) II, (c) III, (d) IV and (e) V

(a) 12UTC01NOV1997

(b) 00UTC02NOV1997

(c) 12UTC02NOV1997

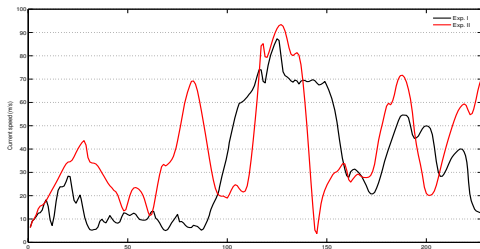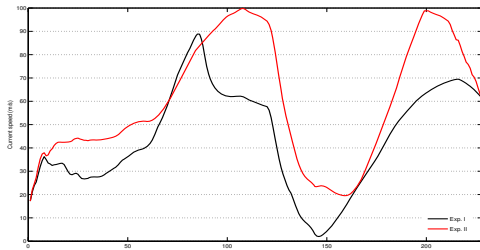(d) 00UTC03NOV1997

(e) 12UTC03NOV1997

Fig. 5.   Current speed ($cm\ s^{-1}$) and its direction in the Exp. I at the stations (a) I, (b) II, (c) III, (d) IV and (e) V
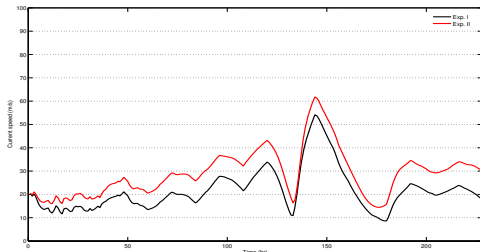
(a) 12UTC01NOV1997

(b) 00UTC02NOV1997

(c) 12UTC02NOV1997

(d) 00UTC03NOV1997
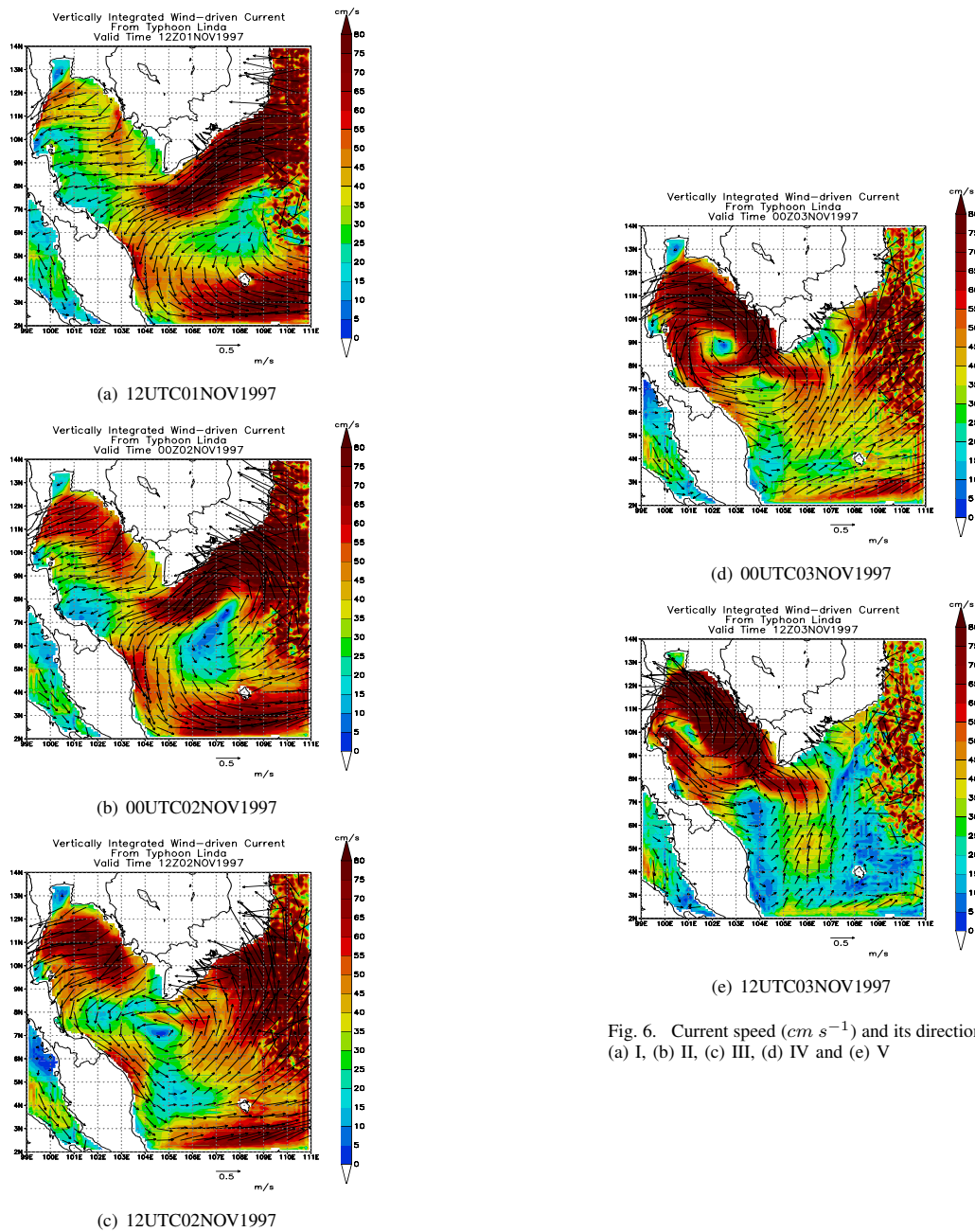
(e) 12UTC03NOV1997

Fig. 6. Current speed ($cm\ s^{-1}$) and its direction in the Exp. II at the stations (a) I, (b) II, (c) III, (d) IV and (e) V
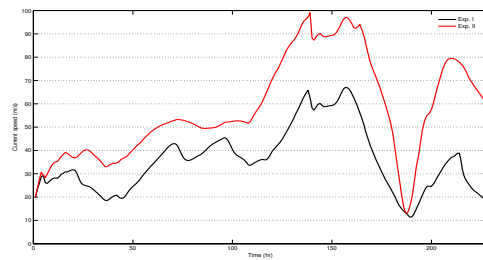
772
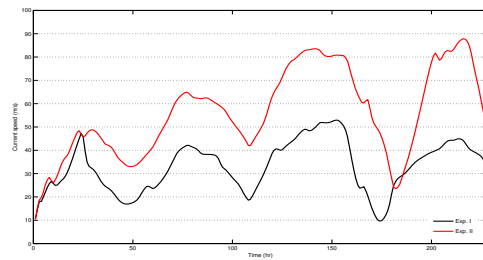
(a) 12UTC01NOV1997

(b) 00UTC02NOV1997

(c) 12UTC02NOV1997

(d) 00UTC03NOV1997

(e) 12UTC03NOV1997

Fig. 7.   Current speed in the Exp. I and II at each station during 0000 UTC on October 28, 1997 to 1200 UTC on November 6, 1997